TRK Fusions Are Enriched in Cancers with Uncommon Histologies and the Absence of Canonical Driver Mutations

Ezra Y. Rosen[1], Debra A. Goldman[2], Jaclyn F. Hechtman[3], Ryma Benayed[3], Alison M. Schram[1,4], Emiliano Cocco[5], Sophie Shifman[5], Yixiao Gong[6], Ritika Kundra[6], James P. Solomon[3], Alberto Bardelli[7,8], Maurizio Scaltriti[3,5], Alexander Drilon[1,4], Alexia Iasonos[2,4], Barry S. Taylor[2,4,5,6], and David M. Hyman[1,4]

ABSTRACT

Purpose: TRK inhibitors achieve marked tumor-agnostic efficacy in TRK fusion–positive cancers and consequently are now an established standard of care. Little is known, however, about the demographics, outcomes, response to alternative standard therapies, or genomic characteristics of TRK fusion–positive cancers.

Experimental Design: Utilizing a center-wide screening program involving more than 26,000 prospectively sequenced patients, genomic and clinical data from all cases with TRK fusions were extracted. An integrated analysis was performed of genomic, therapeutic, and phenomic outcomes.

Results: We identified 76 cases with confirmed TRK fusions (0.28% overall prevalence) involving 48 unique rearrangements and 17 cancer types. The presence of a TRK fusion was associated with depletion of concurrent oncogenic drivers ($P < 0.001$) and lower tumor mutation burden ($P < 0.001$), with the exception of colorectal cancer where TRK fusions cooccur with microsatellite instability (MSI-H). Longitudinal profiling in a subset of patients indicated that TRK fusions were present in all sampled timepoints in 82% (14/17) of cases. Progression-free survival on first-line therapy, excluding TRK inhibitors, administered for advanced disease was 9.6 months [95% confidence interval (CI), 4.8–13.2]. The best overall response rate achieved with chemotherapy containing–regimens across all lines of therapy was 63% (95% CI, 41–81). Among 12 patients treated with checkpoint inhibitors, a patient with MSI-H colorectal cancer had the only observed response.

Conclusions: TRK fusion–positive cancers can respond to alternative standards of care, although efficacy of immunotherapy in the absence of other predictive biomarkers (MSI-H) appears limited. TRK fusions are present in tumors with simple genomes lacking in concurrent drivers that may partially explain the tumor-agnostic efficacy of TRK inhibitors.

Introduction

The *NTRK* genes (*NTRK1/2/3*) encode the family of TRK receptor tyrosine kinases (TrkA/B/C) that play a critical role in neuronal homeostasis during embryonic development (1, 2). Following birth, TRK expression is primarily limited to the nervous system where these kinases are involved in pain sensing, memory, weight homeostasis, and proprioception (3, 4). TRK is the target of recurrent fusion events across a wide variety of pediatric and adult cancers where they behave as classic oncogenic drivers (5–7). TRK inhibitors have demonstrated dramatic and durable tumor-agnostic efficacy in TRK fusion–positive cancers (8–10). For the first time in oncology therapy, TRK inhibitors larotrectinib and entrectinib are now FDA approved for the treatment of any advanced TRK fusion–positive pediatric or adult solid tumor (11).

Despite the significant progress in treating TRK fusion–positive cancers, many important questions remain. The true frequency and distribution of TRK fusions within and across cancer types remains poorly defined. Similarly, the diversity and key features of TRK fusions themselves, as well as their broader genomic context in affected tumors, remain uncertain. Perhaps most importantly, the natural history and response to alternative (non-TRK inhibitor) standards of care for TRK fusion–positive cancers is unknown. Answering these critical and unresolved questions has been challenging due to the extreme rarity, broad distribution across cancer types, and technical limitations of detection of TRK fusions.

To address these knowledge gaps, we conducted an integrated analysis of the clinical and genomic features of all TRK fusion–positive cancers detected at our center leveraging a large multi-year effort to prospectively genomically characterize patients (12, 13). To our knowledge, this cohort of TRK fusion–positive cancers represents the largest deeply annotated cohort assembled to date, exceeding the size of the pivotal larotrectinib dataset itself. Here, we present the detailed natural history, disease course, and prognosis of patients with TRK-driven cancers with the goal of further informing diagnostic and treatment decisions.

Materials and Methods

Patients and sequencing

All pediatric and adult patients with TRK fusion–positive cancers identified at Memorial Sloan Kettering (MSK) between April 7, 2015 and August 15, 2018 were included for analysis under an Institutional review board–approved retrospective research protocol. Patients were

[1]Department of Medicine, Memorial Sloan Kettering, New York, New York. [2]Department of Epidemiology and Biostatistics, Memorial Sloan Kettering, New York, New York. [3]Department of Pathology, Memorial Sloan Kettering, New York, New York. [4]Weill Cornell Medical College, New York, New York. [5]Human Oncology and Pathogenesis Program, Memorial Sloan Kettering, New York, New York. [6]Marie-Josée and Henry R. Kravis Center for Molecular Oncology, Memorial Sloan Kettering, New York, New York. [7]Candiolo Cancer Institute FPO-IRCCS, Candiolo, Italy. [8]Department of Oncology, University of Torino, Candiolo, Italy.

Note: Supplementary data for this article are available at Clinical Cancer Research Online (http://clincancerres.aacrjournals.org/).

Corresponding Author: David M. Hyman, Current address, Loxo Oncology, 281 Tresser Blvd., 9th Floor, Stamford, CT 06901. E-mail: dhyman@loxooncology.com

Clin Cancer Res 2020;26:1624–32

doi: 10.1158/1078-0432.CCR-19-3165

Translational Relevance

The global tumor-agnostic regulatory approval of TRK inhibitors for any pediatric or adult cancer harboring this biomarker establishes TRK fusion–positive cancer as a new diagnostic entity of which relatively little is known. These data provide an initial comprehensive clinicopathologic and genomic overview of TRK fusion–positive cancers. Although the heterogeneity of TRK fusion–positive cancers prevented a formal comparison, we did not find clear evidence that TRK fusion–positive cancers have an unexpectedly favorable prognosis. To further enhance the value of this analysis and facilitate additional outcome analyses, patient-level treatment and genomic data have also been made available to the broader research community.

characterized as harboring TRK fusions on the basis of DNA-based hybrid-capture next-generation sequencing (MSK-IMPACT; ref. 14) or targeted RNA sequencing using anchored multiplex PCR technology (MSK-Fusion; ref. 15). Three MSK-IMPACT assay versions were used (version 1, 310 genes; version 2, 410 genes; version 3, 468 genes). Beginning with MSK-IMPACT version 3, select tiling of *NTRK1* introns 3, 7, 8, 9, 10, 11, and 12, *NTRK2* intron 15, and *ETV6* introns 4 and 5, a common upstream TRK fusion partner, were added. Thus, MSK-IMPACT version 3 was similarly capable of detecting of select *NTRK1* or *NTRK2* fusions, as well as *NTRK1/2/3* fusions involving upstream partners with intronic tiling (ETV6). Patients were tested by MSK-IMPACT either as part of routine care or via an institution-wide perspective genotyping protocol (ClinicalTrials.gov, NCT01775072) as described previously (13).

The RNA-based MSK-Fusion assay covered *NTRK1* exons 8, 10, 11, 12, 13, and 14, *NTRK2* exons 11–18, and *NTRK3* exons 13–16, which included the critical kinase domain exons. The testing methodology utilized a universal adapter design (ArcherDx) and permits detection of any upstream fusion partner involving included NTRK exons. Thus, MSK-Fusion was expected to have a high sensitivity for any expressed TRK fusion. MSK-Fusion was performed reflexively in cases where MSK-IMPACT testing identified structural rearrangements of uncertain significance involving *NTRK1/2/3*. Similarly, the test was performed selectively in cases where MSK-IMPACT detected no mitogenic driver, especially in tumor types known to harbor recurrent fusion events (i.e., lung, thyroid, and biliary cancers). Finally, MSK-Fusion was utilized for cancers where fusion detection is important for pathologic diagnosis, including select sarcomas.

In cases of secretory carcinoma of the breast or salivary gland, which have near obligate *ETV6-NTRK3* fusions (16), *ETV6* DNA-level rearrangement demonstrated by break-apart FISH was also accepted as inferred evidence of a TRK fusion.

All potential TRK fusions were manually curated to ensure they were in-frame and predicted to result in a fusion transcript. Patients with TRK fusions identified by MSK-IMPACT, but negative by MSK-Fusion were considered TRK-negative. In select cases involving novel upstream TRK fusion partners, or where it was challenging to determine the reading frame, pan-TRK IHC was performed using previously described methods (17, 18).

All cases with qualifying TRK fusions underwent detailed clinical data curation from the electronic medical record. Baseline demographic, pathologic, and clinical data from the date of presentation were extracted. All cases underwent pathologic review at MSKCC by expert pathologists based on disease type. All surgical, radiologic, and medical therapies for disease were captured including best response, where applicable, as determined by the treating physician. Estimates of TRK fusion positivity by disease were calculated using patients for whom there were either MSK-IMPACT or MSK-Fusion data, and the two TRK-positive patients with FISH data only were excluded from this analysis (Supplementary Fig. S1). We used the Wilcoxon rank sum and Fisher exact test to examine the association between TRK fusion with TMB and any oncogenic driver, respectively.

Genomic analysis

All genomic analyses were performed using the R programming language and environment (https://www.r-project.org), and Circos plots were generated using the RCircos library. Fusion breakpoints were determined using genomic coordinates as determined by MSK-IMPACT, or when those data were unavailable, using the exon breakpoints called by MSK-Fusion. OncoPrints were generated using the cBioPortal (https://www.cbioportal.org/). In patients with multiple sequenced samples, the earliest sequenced sample demonstrating a TRK fusion was utilized for analysis. Tumor mutation burden (TMB) was calculated using the mutations called by MSK-IMPACT using previously published methods (19). TMB was compared in all patients with MSK-IMPACT to TRK-positive patients excluding patients with MSI-high colorectal cancer. These patients were excluded as they are known to be enriched. Wilcoxon rank sum and Fisher exact test were used to examine the association between TRK fusion with TMB and any oncogenic driver, respectively.

Statistical analysis

Recurrence-free survival (RFS), progression-free survival (PFS), and overall survival (OS) were estimated using Kaplan–Meier methods. OS was assessed from original diagnosis until death from any cause. Patients alive at the time of the data lock (January 23, 2019) were censored at the last date confirmed alive. For RFS, patients treated with curative intent ($n = 39$) were included. We defined this as patients who were treated with curative intent and nonexploratory surgery for whom date of start of remission was their surgery date, and 1 patient with curative intent chemotherapy and surgery for whom date of remission was date of first imaging study showing no evidence of disease. Patients were excluded from RFS analysis if not treated with curative intent ($n = 17$), no documentation ($n = 8$), or if never in remission ($n = 12$). Of patients included in RFS analysis ($n = 39$), recurrence was documented on imaging in 27 patients. RFS was calculated from the start of remission until first recurrence or death from any cause. Patients alive without radiologic or pathologic documentation of recurrence were censored at last follow up. PFS was defined from date of first-line therapy for advanced disease (time 0) until radiologic progression ($n = 37$), changing therapies to start a clinical trial ($n = 2$), or changing medical therapies for other reasons ($n = 4$). For PFS, patients who developed advanced disease or with *de novo* metastatic disease were included ($n = 51$). Patients were excluded if they had curative first-line treatment and remained disease free at time 0 ($n = 13$), with incurable disease but never treated with systemic therapy for this condition ($n = 4$), and those with inadequate records ($n = 8$). PFS was defined from date of first-line therapy for advanced disease (time 0) until radiologic progression ($n = 37$), changing therapies to start a clinical trial ($n = 2$), or changing medical therapies for other reasons ($n = 4$). Patients alive and progression-free at the time of data cut were censored at last follow-up. Ninety-five percent confidence intervals (95% CI) around survival estimates were calculated with the log-cumulative hazard transformation.

For patients who received therapy in the setting of active disease, best overall response was recorded when available as indicated by the treating oncologist. We calculated best overall response to any therapy, first-line therapy, and by drug classification (chemotherapy, immunotherapy, and TRK-targeted therapy) with 95% Clopper–Pearson CIs. Patients who received TRK inhibitors as first-line therapy were not included in first-line assessment, and patients who received multiple agents may be counted in both drugs' assessment.

To estimate the frequency of TRK fusions by cancer type, the number of TRK fusion–positive cases in each cancer type over the total number of patients with that tumor type tested for TRK fusions via MSK-IMPACT (v.2 and 3) or MSK-Fusion was calculated. Tumor types were classified using the OncoTree ontology (http://oncotree.mskcc.org/). Ninety-five percent CIs were calculated by the Clopper–Pearson method. Finally, percent agreement between MSK-IMPACT and MSK-Fusion for patients that had both assays performed ($N = 46$) was calculated. All analyses were performed with SAS 9.4 (The SAS Institute).

Cell culture experiments

The *LMNA-NTRK1* colorectal cancer cell line was obtained from Dr. Alberto Bardelli (Candiolo Cancer Institute, FPO, IRCCS, Turin, Italy). The *GON4L-NTRK1,* NRAS Q61R cell line was established from a PDX engrafted with a biopsy of a patient with larotrectinib-naïve melanoma. Larotrectinib, LOXO-195, and trametinib were purchased from Selleckchem. RNA was isolated from the *GON4L-NTRK1, NRAS* Q61R melanoma cell line using the QIAGEN RNeasy kit and cDNA synthesis was made using the Bio-Rad cDNA synthesis kit. The amplicon including the breakpoint of the *GON4L-NTRK1* fusion was amplified with the following primers: forward: 5′ GCTTCAACCCTGGGAAAACACC 3′; reverse: 5′ AAGAGGCAGGCAAAGACG 3′. PCR was performed with a VERITI 96 Well Thermal Cycler (Applied Biosystems). CellTiter Glo-based assay was used to evaluate the effect of drug on the proliferation of the *GON4L-NTRK1, NRAS* Q61R cell line. Cells were seeded, and the following day larotrectinib, LOXO-195 or trametinib (1:2 dilutions starting with a maximum concentration of 1,000 nmol/L) was added. CellTiter Glo reagent was added 72 hours later and absorbance was read at 490 nm. For Western blotting, the *GON4L-NTRK1, NRAS* Q61R melanoma cell line was plated, and the day after larotrectinib (50 nmol/L), LOXO-195 (50 nmol/L), or trametinib (20 nmol/L) were added. Twenty-four hours later, lysates were collected. Antibodies used in the assay were the following: pan-Trk clone A7H6R (92991S, Cell Signaling Technology), phospho p44/42 MAPK (Erk1/2; T202/Y204) clone D13.14.4E (4370S, Cell Signaling Technology), phospho MEK1/2 (S217/221) clone 41G9 (9154S, Cell Signaling Technology), and vinculin clone E1E9V (13901S, Cell Signaling Technology). Protein lysates extracted from the *LMNA-NTRK1* CRC cell line were loaded as control.

Data availability

Patient-level clinical and genomic data are available publically at the CBioPortal (https://www.cbioportal.org/study/summary?id=ntrk_msk_2019).

Results

Patient characteristics

In total, 76 patients had confirmed TRK fusions representing 17 distinct tumor types (**Table 1**). As expected, tumor types known to be enriched for TRK fusions were most frequently represented including salivary (predominantly secretory carcinoma), sarcoma, and thyroid. More common tumor types also known to infrequently harbor TRK fusions including colon, lung, melanoma, pancreas, breast cancer, and glioma were also observed. Patients presented with a mixture of early (45%) and late (55%) stage disease. The median age was 52 (range: 1 week–78 years; Supplementary Fig. S2).

Table 1. Patient demographics.

Factor[a]	*N* (%)
Age, median (range)	52 (0–78)
Gender	
Female	47 (61.8)
Male	29 (38.2)
Cancer type	
Salivary	12 (15.8)
Thyroid	10 (13.2)
Sarcoma NOS	9 (11.8)
Colon	8 (10.5)
Lung	6 (7.9)
Melanoma	5 (6.6)
Glioblastoma multiforme	4 (5.3)
Pancreatic cancer	4 (5.3)
Other	18 (23.7)
Stage at diagnosis ($n = 58$)	
Localized, I–III	34 (58.6)
Metastatic, IV	24 (41.4)
Prior therapy	
Surgery ($n = 74$)	65 (87.8)
Radiation ($n = 70$)	33 (47.1)
Systemic ($n = 76$)	57 (75)
Class of systemic therapy ($n = 57$)	
Chemotherapy	39 (68.4)
Immunotherapy	12 (21.1)
TRK-Targeted therapy	39 (68.4)
Intervals, years, median (range)	
Diagnosis and TRK tissue ($N = 72$)	0.2 (0.0–21.4)
Diagnosis and NTRK sequencing ($N = 75$)	2.0 (0.0–21.6)
TRK Tissue and sequencing ($N = 72$)	0.3 (0.0–13.0)

Note: Table showing patient demographics, including age, gender, cancer type, stage, treatment received, and timing of detection of TRK fusion.
[a]$N = 76$ for all factors unless otherwise noted.

TRK fusions were identified from both primary (47%, 36/76) and metastatic (53%, 40/76) samples. TRK fusions were detected through a variety of assays including both DNA and RNA ($n = 34$), DNA alone ($N = 19$), RNA alone ($N = 21$), and FISH alone ($N = 2$). In 26% (12/46) of cases where both DNA and RNA were assayed, DNA testing did not detect TRK fusions ultimately identified by RNA sequencing. All of these discordant cases involved introns of *NTRK2/3* that could not be feasibly included in the MSK-IMPACT design due to their size, representing a known limitation of DNA-based TRK fusion detection in general (18, 20). Conversely, all in-frame TRK fusions detected by DNA testing were confirmed by RNA testing.

TRK fusions

The overall prevalence of TRK fusions during the study period was 0.28% (74/26,312), with the rates varying significantly by cancer type (**Table 2**). The highest frequency of TRK fusions was observed in salivary cancers (5.29%, 95% CI, 2.76%–9.05%), reflecting the near pathognomonic presence of *ETV6-NTRK3* fusions in mammary

Table 2. Prevalence of TRK fusions overall and by cancer type.

Histology	Percent	95% CI	Fraction
Overall	0.28%	(0.22%–0.35%)	74/26,312
Salivary carcinoma	5.29%	(2.76%–9.05%)	12/227
Thyroid cancer	2.22%	(1.07%–4.04%)	10/451
Sarcoma NOS	1.17%	(0.54%–2.21%)	9/770
Uterine sarcoma	1.15%	(0.14%–4.09%)	2/174
Glioblastoma multiforme	0.62%	(0.17%–1.59%)	4/641
Appendiceal adenocarcinoma	0.57%	(0.01%–3.12%)	1/176
Melanoma	0.54%	(0.17%–1.25%)	5/932
Biliary tract cancer	0.36%	(0.04%–1.30%)	2/553
Unknown primary	0.31%	(0.01%–1.74%)	1/318
Colon cancer	0.35%	(0.15%–0.68%)	8/2,306
Pancreatic cancer	0.30%	(0.08%–0.78%)	4/1,315
Lung adenocarcinoma	0.16%	(0.06%–0.36%)	6/3,658
Invasive breast carcinoma[a]	0.08%	(0.02%–0.23%)	3/3,775

[a]Excludes secretory breast cancer.

analogue secretory carcinomas that accounted for 11 of 12 salivary cases. The remaining *ETV6-NTRK3*-containing salivary tumor underwent pathologic reexamination again confirming the diagnosis of salivary duct carcinoma and excluding secretory carcinoma on the basis of both classic morphology and compatible IHC profile (negative S100), suggesting that molecular screening of salivary tumors without classic secretory carcinoma features may still be warranted. TRK fusions were next most commonly found in thyroid carcinomas and sarcomas (both soft tissue and uterine). In the remainder of the cohort, point estimates for the frequency of TRK fusions were $\leq 1\%$. In breast cancer, after excluding secretory histology that harbor near pathognomonic *ETV6-NTRK3* rearrangements (21), only 0.08% of cases (3/3,775) were TRK fusion–positive. Also of note, despite sequencing of greater than 1,561 patients with prostate cancer during the study period, none were identified as TRK fusion–positive.

With the adoption of genome-driven basket studies and tumor-agnostic therapies (22), one outstanding question is the degree to which the patient population enrolled in pivotal development programs reflected the broader population of patients whose tumors harbor these biomarkers. To evaluate this, the distribution of tumor types observed in patients enrolled in the larotrectinib development program (10) was compared with the MSK cohort (Supplementary Fig. S3). For this analysis, patients with primary central nervous system tumors were excluded from the MSK cohort as they were not included in the comparable larotrectinib dataset. Overall, the distribution of cancer types was broadly similar between the two cohorts with some notable exceptions. Infantile fibrosarcoma, a tumor type with pathognomonic *ETV6-NTRK3* fusions (23, 24), was enriched in the larotrectinib cohort. This was likely due to intensification of TRK fusion screening in this rare patient population by the pediatric oncology community due to both high unmet need and the dramatic efficacy of TRK inhibition in this subset (9). In comparison, colorectal and pancreatic cancers were observed more frequently in the MSK compared with larotrectinib cohorts, potentially reflecting nearly universal use of broad next-generation testing in these patient populations at MSKCC. Finally, four cases of gastrointestinal stromal tumors (GIST) were observed in the larotrectinib dataset, but were not present at all in the MSK cohort. Despite these noteworthy differences, these data could suggest that the study cohort enrolled in the pivotal larotrectinib development program may be broadly reflective of how this agent is used in the postmarketing setting.

Genomic analysis

The majority of *NTRK1* fusions involved intrachromosomal upstream partners, while only a minority of *NTRK2* fusions and no *NTRK3* fusions were intrachromosomal (**Fig. 1A**). Subsequent analysis of intrachromosomal *NTRK1* fusions (**Fig. 1B**) suggested that unlike fusions in prostate cancers like TMPRSS2-ERG (25), these events were not the result of an interstitial deletion. In total, 48 unique fusion events were observed (**Fig. 1C**; Supplementary Table S1). Overall, *TERT* promoter, *TP53*, and *NOTCH1/2* gene mutations were the most common coalterations in this cohort (Supplementary Table S2). Consistent across all fusions was inclusion of the full-length kinase domain of *NTRK*1/2/3, suggesting that this feature should be an important part of the evaluation of any potential novel TRK fusion. The most common upstream fusion partner was *ETV6* followed by *EML4*, both of which were observed exclusively in the context of *NTRK3*. In comparison with *NTRK3, NTRK1/2* did not have any single preferred upstream fusion partner.

The comutational patterns were compared in the TRK fusion–positive cases in which broader profiling was available ($n = 65$) and TRK fusion–negative cases prospectively sequenced during the same time period ($n = 25{,}989$). Whereas 31.4% of TRK fusion–negative cases harbored activating alterations in select canonical MAPK pathway oncogenes, a similar pattern of coalteration was only observed in 1.5% (1 patient) of TRK fusion–positive cases (**Fig. 1D**). Interestingly, this patient with melanoma with concurrent *GON4L-NTRK1* and *NRAS* Q61R alterations was one of only 6 patients in the pivotal larotrectinib dataset to experience progressive disease as their best response (26). To investigate this case further, we confirmed with RT-PCR the presence of the GON4L-NTRK1 fusion initially detected in DNA (Supplementary Fig. S4A and S4B). However, pan-TRK IHC staining was negative, suggesting this transcript was not expressed at the protein level (Supplementary Fig. S4C). Moreover, a cell line derived from this patient's tumor was insensitive to larotrectinib or the next-generation TRK inhibitor LOXO-195, but responsive to trametinib (Supplementary Fig. S4D). Consistent with this, Western blots confirmed absence of TRK expression as well as reduction of pERK with trametinib. (Supplementary Fig. S4E). Collectively, these data suggest that TRK fusions only infrequently cooccur with other canonical alterations in therapy-naïve patients, but in the rare cases where they do these tumors may not exhibit oncogenic dependence on the TRK fusion.

To further interrogate the genomic context in which TRK fusions arise, the TMB of TRK fusion–positive and negative cases were compared. The acquisition of kinase fusions including TRK has been previously associated with the presence of MSI in colorectal cancers (27, 28). Indeed, of cases where MSI testing was available, 86% (6/7) of TRK fusion–positive colorectal cancers were microsatellite high (MSI-H). In comparison, no other TRK fusion–positive cancer was MSI-H. Excluding these MSI-H colorectal cancers, median TMB was lower in the TRK fusion–positive versus negative cases (1.8 vs. 3.5, $P < 0.001$; **Fig. 1E**). This association held even when the comparison between mutation count was restricted to alterations classified as either oncogenic or occurring at previously established hotspots (median 1 vs. 2, $P < 0.001$).

As the persistence of TRK fusions over time is unknown, we examined the molecular results from 17 patients in whom more than one tumor sample was evaluated. In 82% (14/17) of cases the TRK fusion was detected in all sequenced time points. Two of the discordant cases were patients with breast cancer in whom the TRK fusions were identified in metastatic but not primary samples (Supplementary Fig. S5A and S5B). The third discordant case was a patient with

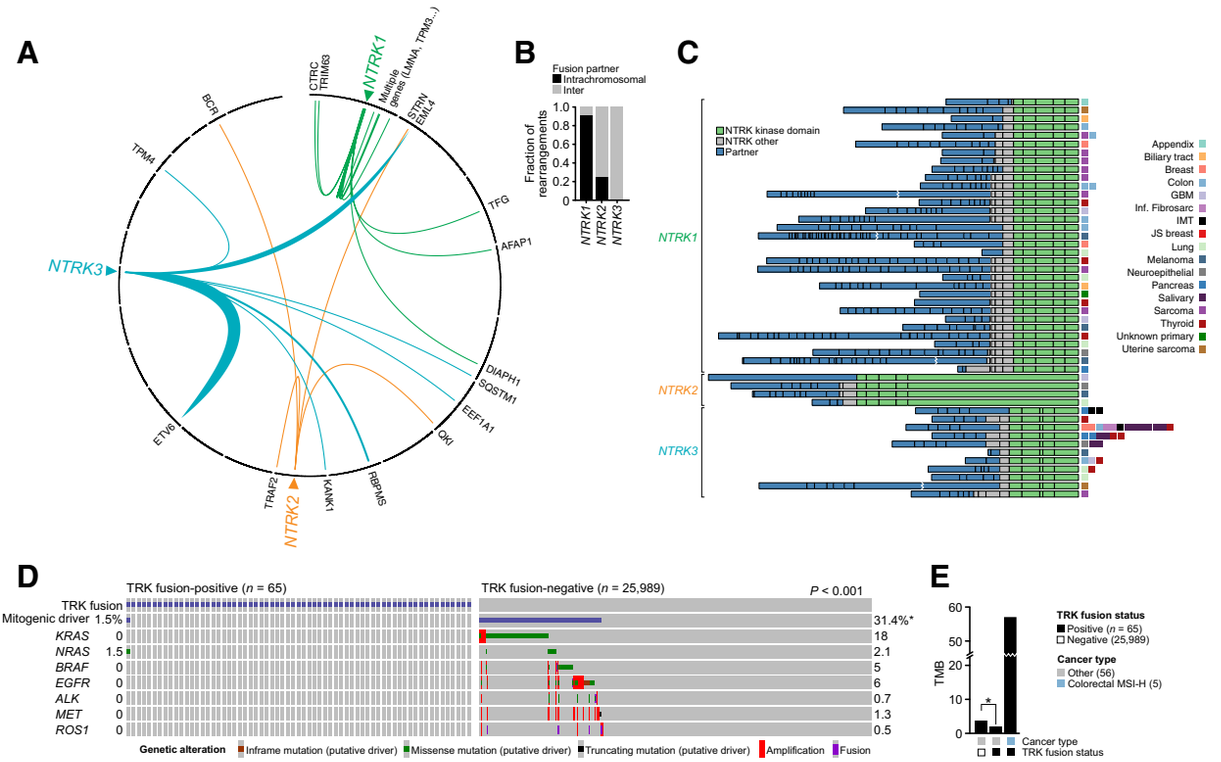

Figure 1.

Genomic characteristics of TRK fusion–positive cancers. **A** and **B,** Circos plots graphically depicting TRKs and their fusion partners, showing intrachromosomal preference for fusion partner for *NTRK1*, but no such preference for *NTRK2* or *NTRK3*. **C,** Schematic of all TRK fusion proteins identified by either MSK-IMPACT or MSK-Fusion, at scale with exons represented by individual boxes. The upstream partner is colored blue, with TRK kinase domain colored green and other TRK exons colored gray. **D,** Oncoprint of TRK-positive versus TRK-negative tumors showing rarity of cooccurrence of TRK fusion with other canonical oncogenes. **E,** Median TMB of TRK fusion–negative tumors, TRK fusion tumors excluding MSI-H, and MSI-H TRK fusions. TMB of TRK-positive tumors was significantly less (Wilcoxon rank sum, $P < 0.001$) than TRK fusion–negative tumors, with the exception of MSI-H colorectal cancers.

glioblastoma with a *TPM3-NTRK1* fusion identified from his primary surgical debulking procedure obtained prior to treatment with radiation or temozolomide therapy. Upon subsequent progression following upfront combined modality therapy, he was treated with a brain-penetrant TRK inhibitor with progression as best response at 12 weeks. Repeat operative resection and profiling at the time progression demonstrated loss of the TRK fusion and acquisition of a new focal *EGFR* amplification (19.6-fold), potentially consistent with the outgrowth of a new clone under selective therapy of TRK inhibition (Supplementary Fig. S5C).

Treatment outcomes

Of the 76 patients with TRK fusion-positive cancers, 67% (51/76) developed advanced or recurrent disease during the study period and all these patients received systemic therapy (median prior lines of systemic therapy = 3). Classes of therapy received for advanced disease included chemotherapy (n = 35, 69%), immunotherapy (n = 12, 24%), and TRK inhibitors (n = 38, 75%; Supplementary Fig. S6; **Table 3**). The overall response rate for first-line therapy, across all classes of therapy excluding TRK inhibitors was 46.7% (95% CI: 21.3–73.4; **Table 3**). Broadening to best response across all lines of therapy received for advanced disease, the overall response rate with chemotherapy containing-regimens was 62.5% (95% CI: 40.6–81.2; Supplementary Table S3). In total, 12 patients received immunotherapy, including two MSI-H colorectal cancers, and best overall response was known in nine of these cases (Supplementary Table S4). Only one patient with MSI-H colorectal cancer achieved a complete response lasting 3.5 years that was ongoing at the time of data cut. Consistent with expectations, the overall response rate with TRK inhibitor therapy was 64.7% (95% CI: 46.5–80.3).

To better understand outcomes of TRK fusion–positive cancers as a broader diagnostic category, recurrence-free survival (RFS), progression-free survival (PFS), and overall survival (OS) was analyzed (Supplementary Table S5). Follow-up time in survivors was 3.1 years (range: 0.1–22.5). In total, 39 patients presented with limited stage disease initially managed with curative intent. Among these patients, the median RFS was 3.5 years (95% CI: 2.4–4.9; **Fig. 2A**). Similarly, among the 51 patients who developed recurrent or advanced disease, median PFS on first-line therapy was 9.1 months (95% CI: 4.8–13.1; **Fig. 2B**). Across all 76 patients, the median overall survival from time of initial diagnosis was 19.8 years (95% CI: 9.1–NR; **Fig. 2C**). The timing of events from diagnosis, acquisition of tumor material used for molecular profiling, completion of TRK testing, development of advanced disease, initiation of TRK inhibitor therapy, and death or last follow-up is shown in **Fig. 3**. Overall, the median duration of time from initial diagnosis to acquisition of tumor material used for TRK testing was 3.1 months (range: 0.3–256.7) and to TRK sequencing 2 years (range: 0.0–21.6; **Table 1**).

Table 3. Systemic treatment outcomes in advanced and recurrent disease.

	Type of therapy			
	First-line[a]	**Chemo**	**Immuno**	**Targeted (TRK)**
ORR, % (Responders/Total)	46.70% [7/15]	62.50% [15/24]	11.10% [1/9]	67.60% [23/34]
ORR 95% CI	(21.3%–73.4%)	(40.6%–81.2%)	(0.3%–48.2%)	(49.5%–82.6%)
BOR, *N* (%)	*n* = 44	*n* = 35	*n* = 12	*n* = 38
CR	1 (2.3%)	4 (11.4%)	1 (8.3%)	6 (15.8%)
PR	6 (13.6%)	11 (31.4%)	0 (0%)	17 (44.7%)
SD	2 (4.5%)	4 (11.4%)	3 (25.0%)	9 (23.7%)
PD	6 (13.6%)	5 (14.3%)	5 (41.7%)	2 (5.3%)
Unknown	29 (65.9%)	11 (31.4%)	3 (25.0%)	4 (10.5%)

Abbreviations: BOR, best overall response; CR, complete response; ORR, overall response rate; PD, progressive disease; PR, partial response; SD, stable disease.
[a]Any class, excluding TRK inhibitors.

Discussion

Here we leveraged a multiyear prospective institution-wide prospective tumor sequencing effort to define clinicopathologic and genomic features of TRK fusion–positive cancers. We found that the distribution of cancers was enriched for uncommon histologies with higher rates of TRK fusion positivity in a pattern that was broadly similar to enrollment into the studies demonstrating efficacy of TRK inhibitors. These findings provide additional evidence that pivotal datasets used to support tumor-agnostic approval of TRK inhibitors may closely reflect use of these agents postapproval. Although the heterogeneity of TRK fusion–positive cancers prevented a formal comparison, we also did not find clear evidence that TRK fusion–positive cancers have an unexpectedly favorable prognosis. To further enhance the value of this analysis and facilitate additional outcome analyses, we have made patient-level treatment and genomic data available to the broader research community.

An integrated genomic analysis of this TRK fusion–positive cohort also identified several important findings. Specifically, we found that the presence of a TRK fusion is associated with the absence of alternative oncogenic drivers. Similarly, we found that TRK fusions persisted over time in nearly all patients with repeat molecular testing. Collectively, these data imply that the majority of TRK fusions are both clonal and rarely passenger alterations, biological features that may be at least partially responsible for the dramatic and pan-cancer efficacy of TRK inhibitors. In most tumor types, TRK fusion–positive cancers had lower overall tumor mutation burden, excluding MSI-H colorectal cancers, which we did not include in our analyses, as they are enriched for these alterations. Finally, we identified a number of novel upstream fusion partners, corresponding to tumor types in which these housekeeper genes are typically expressed. This again demonstrates the diagnostic challenges in TRK fusion detection (18, 20, 29, 30), and suggest that even RNA-based methodologies that require prespecification of the upstream fusion partner are likely to miss a proportion of events.

This work has several limitations. First, the heterogeneity of cancer types harboring TRK fusions precluded formal comparison with a control group. As such, this analysis does not permit direct determination of the prognostic implications of TRK fusions or how they may otherwise modify response to standard therapies. Similarly, the underlying heterogeneity of tumor types make interpretation of summary clinical outcome measures such as relapse-free and progression-free survival challenging to interpret. Despite this, TRK fusion-positive cancer increasingly represents a distinct and complementary diagnostic classification. As such, both clinicians and global regulatory agencies have repeatedly sought these data. Underlying tumor-type heterogeneity also makes interpretation of certain genomic analyses challenging. For example, both mutational burden as well as the

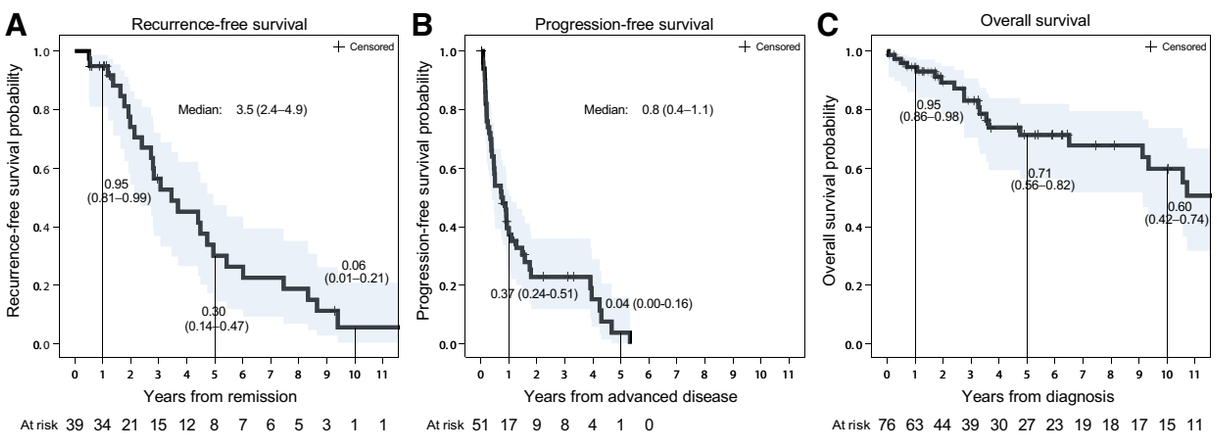

Figure 2
Recurrence-free (**A**), progression-free (**B**), and overall survival (**C**) Kaplan–Meier curves.

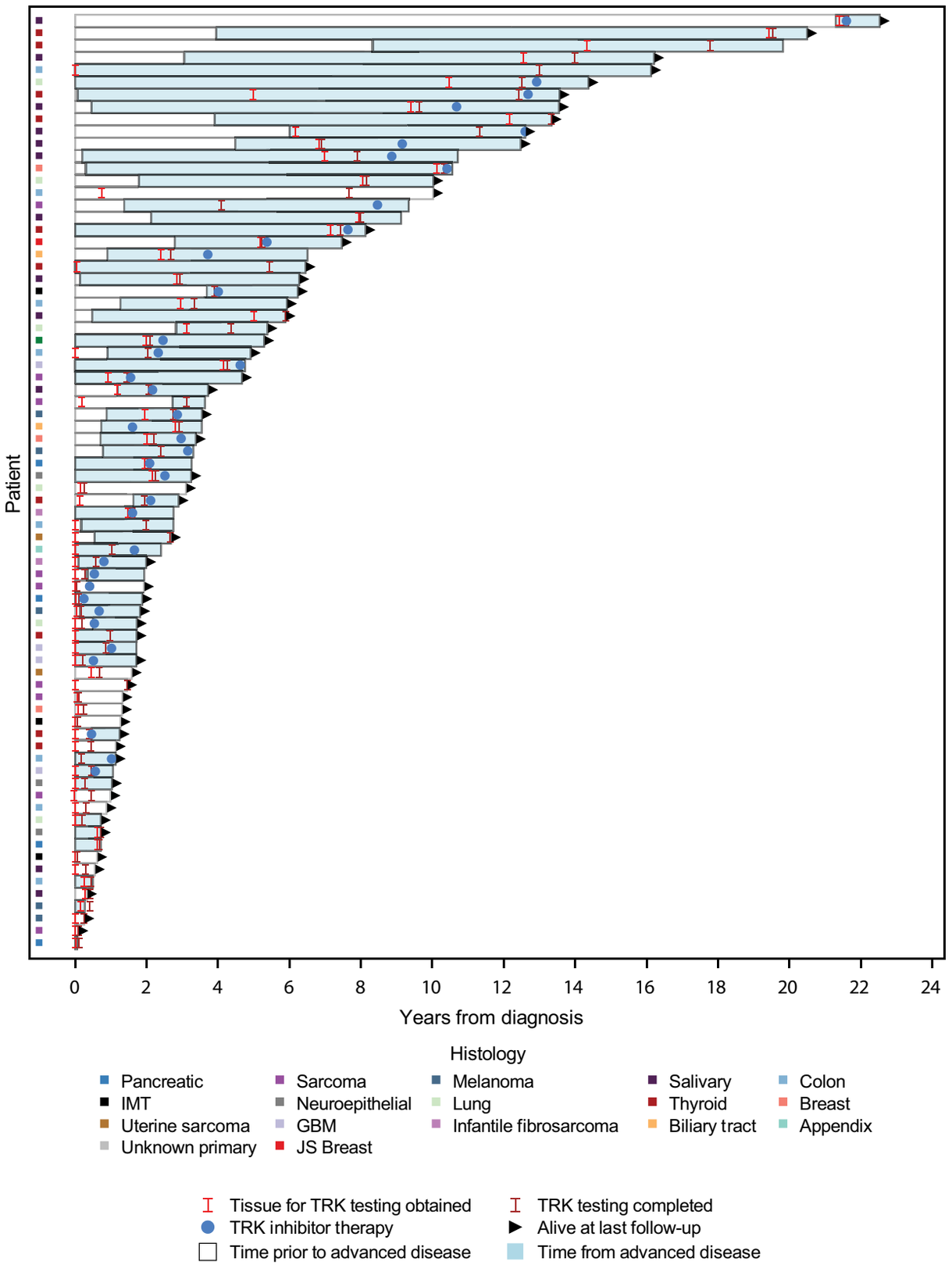

Figure 3.

Patient event plot. Swimmer plot showing timeline of events for all patients, including diagnosis with TRK fusion, time prior to and after the development of advanced disease, time of initiation of TRK inhibitor therapy, and death or last follow-up.

alteration frequency of commonly mutated genes such as *TP53* are closely associated with cancer type. Therefore any comparison of these factors between TRK fusion–positive and negative cohorts is likely to be at least partially confounded by imbalance in the underlying tumor types represented in each group.

Moreover, as with any real-world analysis of a biomarker-defined patient population, TRK fusions were ascertained based on tissue and testing obtained at a variety of different time points relative to each patient's original diagnosis, introducing potential bias in survival estimates. In addition, because the majority of patients (68%) received a TRK inhibitor at some point during the course of their treatment, overall survival measured here likely already reflects the impact of this therapeutic advance. Intriguingly, we also observed a low response rate to immunotherapy. While this finding is noteworthy, we caution that only a small number of TRK fusion–positive patients treated with this therapeutic modality ($n = 12$), especially in cancer types with established sensitivity to checkpoint blockade. Thus, we caution that additional real-world evidence as to the role of immunotherapy in TRK fusion–positive cancers is needed to truly inform patient management. Finally, while our cohort is to our knowledge the most comprehensive of its kind and larger than the pivotal larotrectinib dataset, the study size remains more limited in comparison with more frequent biomarkers. Larger multi-institution efforts (31) will be eventually needed to more fully address these issues.

The global tumor-agnostic regulatory approval of TRK inhibitors for any tumor type harboring this genomic alteration establishes TRK fusion–positive cancer as a new diagnostic entity of which relatively little is known. Through this analysis and patient-level data included, we have begun to define this new entity including insights into the distribution and frequency across cancer types, genomic features, and outcome to existing therapy.

Disclosure of Potential Conflicts of Interest

E.Y. Rosen reports receiving commercial research grants from Bayer. J.F Hechtman is an employee/paid consultant for Medscape and Axiom Health Strategies, and reports receiving commercial research grants from Bayer. R. Benayed reports receiving speakers bureau honoraria from Illumina and Archer. M. Scaltriti reports receiving commercial research grants from Puma Biotechnology, Immunomedics, Targimmune, Daiichi Sankio, and Menarini Ricerche; holds ownership interest (including patents) in Medendi Medical Travel; and is an advisory board member/unpaid consultant for Menarini Ricerche, Daiichi-Sankio, and ADC Pharma. A. Drilon is an employee/paid consultant for Ignyta/Genentech/Roche, Loxo/Bayer/Lilly, Takeda/Ariad/Millenium, TP Therapeutics, AstraZeneca, Pfizer, Blueprint, Helsinn, Beigene, BergenBio, Hengrui, Exelixis, Tyra, Verastem, Abbvie, and MORE Health, and reports receiving other remuneration from GlaxoSmithKline, Teva, Taiho, PharmaMar, Merck, Puma, Wolters Kluwer, Merus, Medscape, OncLive, PeerVoice, Physicians Education Resources, Targeted Oncology, and Research to Practice (CME Honoraria). B.S. Taylor reports receiving other commercial research support and speakers bureau honoraria from Genentech, and other remuneration from Boehringer Ingelheim. D.M. Hyman is an employee/paid consultant for Chugai, Boehringer Ingelheim, AstraZeneca, Pfizer, Bayer, Genentech/Roche, and Fount, and reports receiving commercial research grants from Loxo, Bayer, AstraZeneca, and Puma Biotechnology. No potential conflicts of interest were disclosed by the other authors.

Authors' Contributions

Conception and design: E.Y. Rosen, D.A. Goldman, A.M. Schram, M. Scaltriti, A. Drilon, A. Iasonos, B.S. Taylor, D.M. Hyman

Development of methodology: E.Y. Rosen, J.F. Hechtman, R. Benayed, A.M. Schram, E. Cocco, A. Drilon, A. Iasonos, D.M. Hyman

Acquisition of data (provided animals, acquired and managed patients, provided facilities, etc.): E.Y. Rosen, R. Benayed, A.M. Schram, S. Shifman, J.P. Solomon, A. Drilon, D.M. Hyman

Analysis and interpretation of data (e.g., statistical analysis, biostatistics, computational analysis): E.Y. Rosen, D.A. Goldman, J.F. Hechtman, R. Benayed, A.M. Schram, Y. Gong, R. Kundra, A. Bardelli, M. Scaltriti, A. Drilon, A. Iasonos, B.S. Taylor, D.M. Hyman

Writing, review, and/or revision of the manuscript: E.Y. Rosen, D.A. Goldman, J.F. Hechtman, R. Benayed, A.M. Schram, S. Shifman, R. Kundra, J.P. Solomon, A. Bardelli, M. Scaltriti, A. Drilon, A. Iasonos, B.S. Taylor, D.M. Hyman

Administrative, technical, or material support (i.e., reporting or organizing data, constructing databases): D.M. Hyman

Study supervision: A. Drilon, D.M. Hyman

Acknowledgments

This study was funded by the NCI under the MSKCC Support Grant/Core Grant (P30 CA008748), R01CA226864 (to M. Scaltriti and A. Drilon), NIH 2T32 CA009512-29A1 (to E.Y. Rosen), NIH T32 CA009207 (to A.M. Schram), and ASCO Young Investigator Award (to A.M. Schram). This work was also partially funded by a research grant from Bayer AG, Cycle for Survival, and The Nonna's Garden Foundation Initiative in Precision Oncology.

The costs of publication of this article were defrayed in part by the payment of page charges. This article must therefore be hereby marked *advertisement* in accordance with 18 U.S.C. Section 1734 solely to indicate this fact.

Received September 27, 2019; revised November 14, 2019; accepted December 19, 2019; published first December 23, 2019.

References

1. Nykjaer A, Willnow TE, Petersen CM. p75NTR - Live or let die. Curr Opin Neurobiol 2005;15:49–57.
2. Chao MV. Neurotrophins and their receptors: a convergence point for many signalling pathways. Nat Rev Neurosci 2003;4:299–309.
3. Skaper SD. The neurotrophin family of neurotrophic factors: an overview. Methods Mol Biol 2012;846:1–12.
4. Huang EJ, Reichardt LF. Neurotrophins: roles in neuronal development and function. Annu Rev Neurosci 2001;24:677–736.
5. Mitra G, Martin-Zanca D, Barbacid M. Identification and biochemical characterization of p70(TRK), product of the human TRK oncogene. Proc Natl Acad Sci U S A 1987;84:6707–11.
6. Vaishnavi A, Le AT, Doebele RC. TRKing down an old oncogene in a new era of targeted therapy. Cancer Discov 2015;5:25–34.
7. Khotskaya YB, Holla VR, Farago AF, Mills Shaw KR, Meric-Bernstam F, Hong DS. Targeting TRK family proteins in cancer. Pharmacol Ther 2017;173:58–66.
8. Drilon A, Laetsch TW, Kummar S, DuBois SG, Lassen UN, Demetri GD, et al. Efficacy of larotrectinib in TRK fusion-positive cancers in adults and children. N Engl J Med 2018;378:731–9.
9. Laetsch TW, DuBois SG, Mascarenhas L, Turpin B, Federman N, Albert CM, et al. Larotrectinib for paediatric solid tumours harbouring NTRK gene fusions: phase 1 results from a multicentre, open-label, phase 1/2 study. Lancet Oncol 2018;19:705–14.
10. Lassen UN, Albert CM, Kummar S, van Tilburg SM, Dubois SG, Geoerger B, et al. Larotrectinib efficacy and safety in TRK fusion cancer: an expanded dataset showing consistency in an age and tumor agnostic approach. Ann Oncol 2018;29 Suppl 8:viii133–48.
11. Scott LJ. Larotrectinib: first global approval. Drugs 2019;79:201–6.
12. Hyman DM, Solit DB, Arcila ME, Cheng DT, Sabbatini P, Baselga J, et al. Precision medicine at Memorial Sloan Kettering Cancer Center: clinical next-generation sequencing enabling next-generation targeted therapy trials. Drug Discov Today 2015;20:1422–8.
13. Zehir A, Benayed R, Shah RH, Syed A, Middha S, Kim HR, et al. Mutational landscape of metastatic cancer revealed from prospective clinical sequencing of 10,000 patients. Nat Med 2017;23:703–13.
14. Cheng DT, Mitchell TN, Zehir A, Shah RH, Benayed R, Syed A, et al. Memorial Sloan Kettering Integrated Mutation Profiling of Actionable Cancer Targets (MSK-IMPACT): a hybridization capture-based

next-generation sequencing clinical assay for solid tumor molecular oncology. J Mol Diagn 2015;17:251–64.
15. Benayed R, Offin M, Mullaney K, Sukhadia P, Rios K, Desmeules P, et al. High yield of RNA sequencing for targetable kinase fusions in lung adenocarcinomas with no mitogenic driver alteration detected by DNA sequencing and low tumor mutational burden. Clin Cancer Res 2019;25: 4712–22.
16. Skalova A, Michal M, Simpson RHW. Newly described salivary gland tumors. Mod Pathol 2017;30:S27–S43.
17. Hechtman JF, Benayed R, Hyman DM, Drilon A, Zehir A, Frosina D, et al. Pan-Trk immunohistochemistry is an efficient and reliable screen for the detection of NTRK fusions. Am J Surg Pathol 2017;41:1547–51.
18. Solomon JP, Linkov I, Rosado A, Mullaney K, Rosen EY, Frosina D, et al. NTRK fusion detection across multiple assays and 33,997 cases: diagnostic implications and pitfalls. Mod Pathol 2020;33:38–46.
19. Meléndez B, Van Campenhout C, Rorive S, Remmelink M, Salmon I, D'Haene N. Methods of measurement for tumor mutational burden in tumor tissue. Transl Lung Cancer Res 2018;7:661–7.
20. Marchiò C, Scaltriti M, Ladanyi M, Iafrate AJ, Bibeau F, Dietel M, et al. ESMO recommendations on the standard methods to detect NTRK fusions in daily practice and clinical research. Ann Oncol 2019;30: 1417–27.
21. Krings G, Joseph NM, Bean GR, Solomon D, Onodera C, Talevich E, et al. Genomic profiling of breast secretory carcinomas reveals distinct genetics from other breast cancers and similarity to mammary analog secretory carcinomas. Mod Pathol 2017;30:1086–99.
22. Hyman DM, Taylor BS, Baselga J. Implementing genome-driven oncology. Cell 2017;168:584–9.
23. Baghai F, Yazdani F, Etebarian A, Garajei A, Skalova A. Clinicopathologic and molecular characterization of mammary analogue secretory carcinoma of salivary gland origin. Pathol Res Pract 2017;213:1112–8.
24. Davis JL, Lockwood CM, Stohr B, Boecking C, Al-Ibraheemi A, DuBois SG, et al. Expanding the spectrum of pediatric NTRK-rearranged mesenchymal tumors. Am J Surg Pathol 2019;43:435–45.
25. Taylor BS, Schultz N, Hieronymus H, Gopalan A, Xiao Y, Carver BS, et al. Integrative genomic profiling of human prostate cancer. Cancer Cell 2010;18: 11–22.
26. Drilon A, Laetsch TW, Kummar S, DuBois SG, Lassen UN, Demetri GD, et al. Efficacy of larotrectinib in TRK fusion-positive cancers in adults and children. N Engl J Med 2018;378:731–9.
27. Cocco E, Benhamida J, Middha S, Zehir A, Mullaney K, Shia J, et al. Colorectal carcinomas containing hypermethylated MLH1 promoter and wild-type BRAF/KRAS are enriched for targetable kinase fusions. Cancer Res 2019;79:1047–53.
28. Wang J, Yi Y, Xiao Y, Dong L, Liang L, Teng L, et al. Prevalence of recurrent oncogenic fusion in mismatch repair-deficient colorectal carcinoma with hypermethylated MLH1 and wild-type BRAF and KRAS. Mod Pathol 2019; 32:1053–64.
29. Penault-Llorca F, Rudzinski ER, Sepulveda AR. Testing algorithm for identification of patients with TRK fusion cancer. J Clin Pathol 2019;72:460–7.
30. Hsiao SJ, Zehir A, Sireci AN, Aisner DL. Detection of tumor NTRK gene fusions to identify patients who may benefit from tyrosine kinase (TRK) inhibitor therapy. J Mol Diagn 2019;21:553–71.
31. AACR Project GENIE Consortium. AACR project GENIE: powering precision medicine through an international consortium. Cancer Discov 2017;7: 818–31.